

# DNS Study on Turbulence Generation and Sustainance in Late Boundary Layer Transition

Chaoqun Liu, Ping Lu, Manoj Thapa and Yonghua Yan  
University of Texas at Arlington, Arlington, TX 76019, USA.  
Corresponding author: cliu@uta.edu

**Abstract:** This paper serves as a short review of our recent new DNS study on physics of late boundary layer transition. This includes mechanism of the large coherent vortex structure formation, small length scale generation and flow randomization. The widely spread concept “vortex breakdown to turbulence”, which was considered as the last stage of flow transition, is not observed and is found theoretically incorrect. The classical theory on boundary layer transition is challenged and we proposed a new theory with five steps, i.e. receptivity, linear instability, large vortex formation, small length scale generation, loss of symmetry and randomization to turbulence. We have also proposed a new theory about turbulence generation. The new theory shows that all small length scales (turbulence) are generated by shear layer instability which is produced by large vortex structure with multiple level vortex rings, multiple level sweeps and ejections, and multiple level negative and positive spikes near the laminar sub-layers. Therefore, “turbulence” is not generated by “vortex breakdown” but rather positive and negative spikes and consequent high shear layers. “Shear layer instability” is considered as the “mother of turbulence”. This new theory may give a universal mechanism for turbulence generation and sustainance - the energy is brought by large vortex structure through multiple level sweeps not by “vortex breakdown”. The loss of symmetry and randomization are caused by internal property of the boundary layer. The loss of symmetry starts from the second level ring cycle in the middle of the flow field and spreads to the bottom of the boundary layer and then the whole field. More other new physics have also been discussed.

*Keywords:* DNS, Shear Layer Instability, Flow Transition, Vortex Breakdown, Energy cascade, Turbulence.

## Nomenclature

$M_\infty$	= Mach number	$Re$	= Reynolds number
$\delta_{in}$	= inflow displacement thickness	$T_w$	= wall temperature
$T_\infty$	= free stream temperature	$Lz_{in}$	= height at inflow boundary
$Lz_{out}$	= height at outflow boundary		
$Lx$	= length of computational domain along x direction		
$Ly$	= length of computational domain along y direction		
$x_{in}$	= distance between leading edge of flat plate and upstream boundary of computational domain		
$A_{2d}$	= amplitude of 2D inlet disturbance	$A_{3d}$	= amplitude of 3D inlet disturbance
$\omega$	= frequency of inlet disturbance		
$\alpha_{2d}, \alpha_{3d}$	= two and three dimensional streamwise wave number of inlet disturbance		
$\beta$	= spanwise wave number of inlet disturbance	$R$	= ideal gas constant
$\rho$	= ratio of specific heats	$\mu_\infty$	= viscosity

# 1 Introduction

The transition process from laminar to turbulent flow in boundary layers is a basic scientific problem in modern fluid mechanics. After over a hundred of years of study on flow transition, the linear and weakly non-linear stages of flow transition are pretty well understood. However, for late non-linear transition stages, there are still many questions remaining for research. Adrian [1] described hairpin vortex organization in wall turbulence. Wu and Moin [2] reported a new DNS for flow transition on a flat plate and obtained fully developed turbulent flow with structure of forest of ring-like vortices by flow transition at zero pressure gradients. Recently, Guo et al [3] conducted an experimental study for late boundary layer transition in more details. However, turbulence is still covered by a mystical veil in nature after over a century of intensive study. Following comments are made by wikipedia web page at <http://en.wikipedia.org/wiki/Turbulence> "Nobel Laureate Richard Feynman described turbulence as "the most important unsolved problem of classical physics". According to an apocryphal story, Werner Heisenberg was asked what he would ask God, given the opportunity. His reply was: "When I meet God, I am going to ask him two questions: Why relativity? And why turbulence? I really believe he will have an answer for the first." Horace Lamb was quoted as saying in a speech to the British Association for the Advancement of Science, "I am an old man now, and when I die and go to heaven there are two matters on which I hope for enlightenment. One is quantum electrodynamics, and the other is the turbulent motion of fluids. And about the former I am rather optimistic" (Mullin [4]; Davidson [5]).

These comments clearly show that the mechanism of turbulence formation and sustenance is still a mystery for research. Note that both Heisenberg and Lamb were not optimistic for the turbulence study.

In order to get deep understanding the mechanism of the late flow transition in a boundary layer and physics of turbulence, we recently conducted a high order direct numerical simulation (DNS) with 1920x241x128 grid points and about 600,000 time steps to study the mechanism of the late stages of flow transition in a boundary layer at a free stream Mach number 0.5. The code was very well validated by comparison with linear theory, experiment, and other DNS results.

## 1.1 Richardson's vortex and energy cascade theory (1928)

Richardson believed that a turbulent flow is composed by "eddies" of different sizes. The large eddies will be stretching, unstable and breaking up to smaller eddies. These smaller eddies undergo the same process, giving rise to even smaller eddies. This process will continue until reaching a sufficiently small length scale such that the viscosity of the fluid can effectively dissipate the kinetic energy into internal energy. During the process of vortex breakdown, the kinetic energy of the initial large eddy is divided into the smaller eddies.

## 1.2 Kolmogorov assumption (1941)

The classical theory on turbulence was given by Kolmogorov, a famous Russian mathematician. In general, the large scales of a flow are not isotropic, because they are determined by the particular boundary conditions. Agreeing with Richardson, Kolmogorov assumed: in the Richardson's energy cascade, this geometrical and directional information is lost, while the scale is reduced and so that the statistics of the small scales has a universal character: they are statistically isotropic for all turbulent flows when the Reynolds number is sufficiently high. It was assumed that there is no dissipation during the energy transfer from large vortex to small vortex through "vortex breakdown".

## 1.3 Kolmogorov's first and second hypotheses (1941)

Based on his assumption, Kolmogorov [6] further gave very famous theories on smallest length scale, which is later called Kolmogorov scale (first hypothesis), and turbulence energy spectrum (second hypothesis):

$$\eta = \left(\frac{\nu^3}{\epsilon}\right)^{\frac{1}{4}},$$

$$E(k) = C\epsilon^{\frac{2}{3}}\kappa^{-\frac{5}{3}} \text{ and}$$

$$\epsilon = \gamma \left\{ 2 \overline{\left( \frac{\partial u_1}{\partial x_1} \right)^2} + 2 \overline{\left( \frac{\partial u_2}{\partial x_2} \right)^2} + 2 \overline{\left( \frac{\partial u_3}{\partial x_3} \right)^2} + \overline{\left( \frac{\partial u_2}{\partial x_1} + \frac{\partial u_1}{\partial x_2} \right)^2} + \overline{\left( \frac{\partial u_3}{\partial x_2} + \frac{\partial u_2}{\partial x_3} \right)^2} + \overline{\left( \frac{\partial u_1}{\partial x_3} + \frac{\partial u_3}{\partial x_1} \right)^2} \right\}$$

where,  $\eta$  is Kolmogorov scale,  $\nu$  is kinematic viscosity,  $\epsilon$  is the rate of turbulence dissipation,  $E$  is the energy spectrum function,  $C$  is a constant and  $\kappa$  is the wave number. These formulas were obtained by Kolmogorov's hypothesis that the small length scales are determined by  $\nu$  and  $\epsilon$ , and  $E$  is related to  $\kappa$  and  $\epsilon$ . These formulas are unique according to the dimensional analysis (Frisch, [7]).

## 1.4 A short review of study on late boundary layer transition

The transition process from laminar to turbulent flow in boundary layers is a basic scientific problem in modern fluid mechanics. After over a hundred of years of study on flow transition, the linear and weakly non-linear stages of flow transition are pretty well understood (Herbert.[8]; Kachanov. [9]). However, for late non-linear transition stages, there are still many questions remaining for research (Kleiser et al, [10]; Sandham et al, [11]; U. Rist et al [12], Borodulin et al, [13]; Bake et al [14]; Kachanov, [15]; Piller, [16]). Adrian [1] described hairpin vortex organization in wall turbulence, but did not discuss the sweep and ejection events and the role of the shear layer instability. Wu and Moin [2] reported a new DNS for flow transition on a flat plate. They did obtain fully developed turbulent flow with structure of forest of ring-like vortices by flow transition at zero pressure gradients. However, they did not give the mechanism of the late flow transition. The important mechanism of boundary layer transition such as sweeps, ejections, positive spikes, etc. cannot be found from that paper. Recently, Guo et al [3] conducted an experimental study for late boundary layer transition in more details. They concluded that the U-shaped vortex is a barrel-shaped head wave, secondary vortex, and is induced by second sweeps and positive spikes.

In order to get deep understanding the mechanism of the late flow transition in a boundary layer and physics of turbulence, we recently conducted a high order direct numerical simulation (DNS) with 1920x241x128 grid points and about 600,000 time steps to study the mechanism of the late stages of flow transition in a boundary layer at a free stream Mach number 0.5 [17, 18, 19, 20, 21, 22, 23, 24, 25, 26, 27, 28, 29, 30]. The work was supported by AFOSR, UTA, TACC and NSF Teragrid. A number of new observations are made and new mechanisms are revealed in late boundary layer transition (LBLT) including:

- **Mechanism on secondary and tertiary vortex formation**
- **Mechanism on first ring-like vortex formation**
- **Mechanism on second sweep formation**
- **Mechanism on high share layer formation**
- **Mechanism on positive spike formationion**
- **Mechanism on multiple ring formation**
- **Mechanism on U-shaped vortex formation**
- **Mechanism on small length vortices generation**
- **Mechanism on multiple level high shear layer formation**
- **Mechanism of energy transfer paths**
- **Mechanism on symmetry loss or so called "flow randomization"**
- **Mechanism on thickening of turbulence boundary layer**
- **Mechanism of high surface friction of turbulent flow**

A  $\lambda_2$  technology developed by Jeong and Hussain [31] is used for flow visualization.

## 1.5 Different physics observed by our high order DNS

According to our recent DNS, "vortex breakdown" is not observed (Liu et al,[18, 25, 26]). Liu gave a new theory that "turbulence is not generated by vortex breakdown but shear layer instability" (Liu et al, [18, 26]; Lu et al, [28]). As we believe, "**shear layer instability**" is the "**mother of turbulence**".

As Richardson's energy cascade and Kolmogorov's assumption about "vortex breakdown" are challenged, Kolmogorov's assumption that the smallest vortices are statistically isotropic becomes questionable. Since the smallest vortices are generated by the "shear layer instability," which is closely related to the shape of body configuration, they cannot be isotropic.

If all small vortices are generated by "shear layer instability" but not "vortex breakdown", Kolmogorov's first hypothesis will lose the background. The smallest length scales will be related to stability of the weakest unstable "shear layer". This will require a deep study of "shear layer instability" not only "dimensional analysis". The popular "Kolmogorov scale" is based on dimensional analysis. Although dimensional analysis is an engineering tool for quantity estimation, it would not in general give accurate estimation. Actually, there is no one who observed the smallest "Kolmogorov scale". As we show below, the small vortices are not generated by "vortex breakdown", which cannot happen, but "shear layer instability".

## 1.6 Questions to classical theory on boundary layer transition

The classical theory, which considers "vortex breakdown" as the last stage of boundary layer transition on a flat plate, is challenged and the phenomenon of "hairpin vortex breakdown to smaller structures" is not observed by our new DNS (Liu et al, [18, 20, 21]). The so-called "spikes" are actually a process of multi-bridge or multi-ring formation, which is a rather stable large vortex structure and can travel for a long distance.

As experiment is quite expensive and has very limited power in data acquisition, direct numerical simulation (DNS) becomes a more and more important tool to discover physics. The purpose of this work is to find physics of turbulence by direct numerical simulation. The paper is organized as follows: Section I is a background review; Section II shows the case set up and code validation; Section III is our observation and analysis; Section IV is a summary of our new finding; Section V is the conclusions which are made based on our recent DNS.

## 1.7 New theory on boundary layer transition by Liu

Classical theory on boundary layer transition can be described by four stages: 1) Boundary layer receptivity; 2) Linear instability; 3) Non-linear growth; 4) Vortex breakdown to turbulence. Apparently, we disagree with the classical theory on "vortex breakdown to turbulence". The new theory of boundary layer transition can be described by five stages: 1) Boundary layer receptivity; 2) Linear instability; 3) Large vortex structure formation; 4) Small vortices generation; 5) Symmetry loss and "randomization". By the way, the vortex cascade in turbulence given by Richardson, Kolmogorov and others is not observed.

## 1.8 Summary of the new theory on turbulence generation by Liu

The new theory on turbulence formation and sustenance shows that all small length scales (turbulence) are generated by shear layer instability which is produced by large vortex structure with multiple level vortex rings, multiple level sweeps and ejections, and multiple level negative and positive spikes near the laminar sub-layers. Therefore, "turbulence" is not generated by "vortex breakdown" but rather positive and negative spikes and consequent high shear layers. "Shear layer instability" is considered as the "mother of turbulence". This new theory may give a universal mechanism for turbulence generation and sustenance - the energy is brought by large vortex structure through multiple level sweeps.

Of course, the new theory has to be further studied and confirmed. More mathematical and numerical study is needed.

# 2 Case Setup and Code Validation

## 2.1 Case setup

The computational domain is displayed in Figure 1. The grid level is 1920x128x241, representing the number of grids in streamwise (x), spanwise (y), and wall normal (z) directions. The grid is stretched in the normal direction and uniform in the streamwise and spanwise directions. The length of the first grid interval in

the normal direction at the entrance is found to be 0.43 in wall units ( $Y^+=0.43$ ). The parallel computation is accomplished through the Message Passing Interface (MPI) together with domain decomposition in the streamwise direction (Figure 2). The flow parameters, including Mach number, Reynolds number, etc are listed in Table 1. Here,  $x_{in}$  represents the distance between leading edge and inlet,  $L_x, L_y, L_{z_{in}}$  are the lengths of the computational domain in x-, y-, and z-directions, respectively, and  $T_w$  is the wall temperature.

Table 1: Flow parameters

$M_\infty$	$Re$	$x_{in}$	$L_x$	$L_y$	$L_{z_{in}}$	$T_w$	$T_\infty$
0.5	1000	$300.79\delta_{in}$	$798.03\delta_{in}$	$22\delta_{in}$	$40\delta_{in}$	273.15K	273.15K

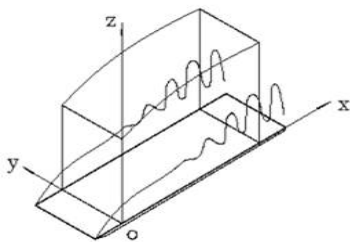


Figure 1: Computation domain.

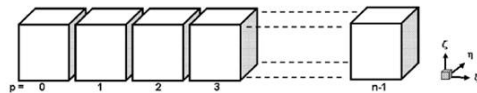


Figure 2: Domain decomposition along the streamwise direction in the computational space.

## 2.2 Code Validation

The DNS code - "DNSUTA" has been validated by NASA Langley and UTA researchers (Jiang et al, [32]; Liu et al, [18]; Lu et al [28]) carefully to make sure the DNS results are correct.

### 2.2.1 Comparison with Linear Theory

Figure 3 compares the velocity profile of the T-S wave given by our DNS results to linear theory. Figure 4 is a comparison of the perturbation amplification rate between DNS and LST. The agreement between linear theory and our numerical results is quite good.

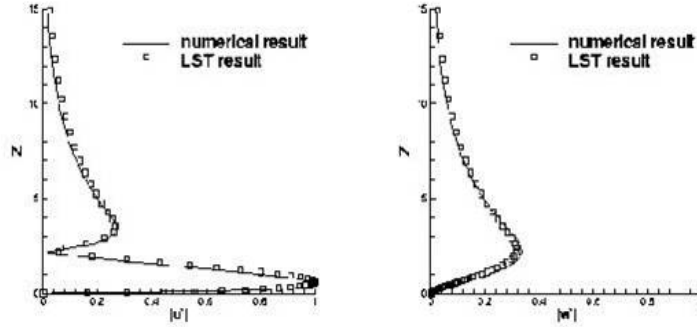


Figure 3: Comparison of the numerical and LST velocity profiles at  $Re_x=394300$ .

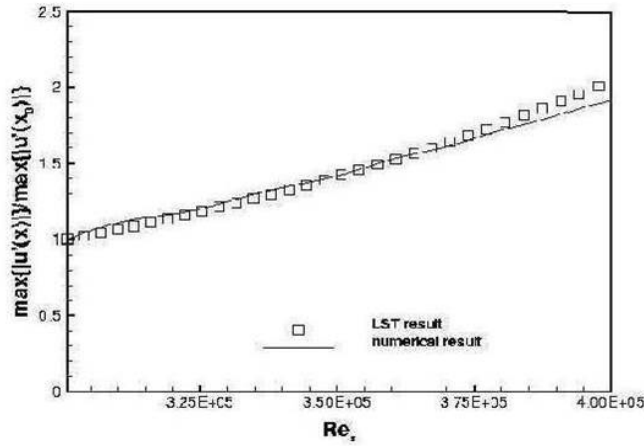


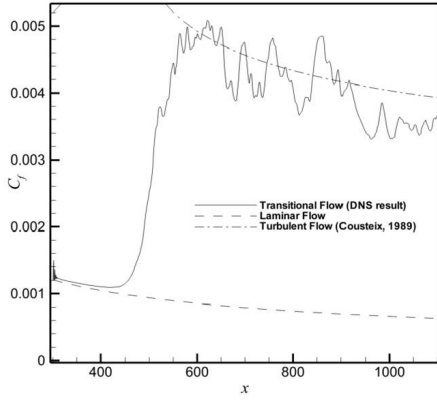
Figure 4: Comparison of the perturbation amplification rate between DNS and LST.

### 2.2.2 Grid Convergence

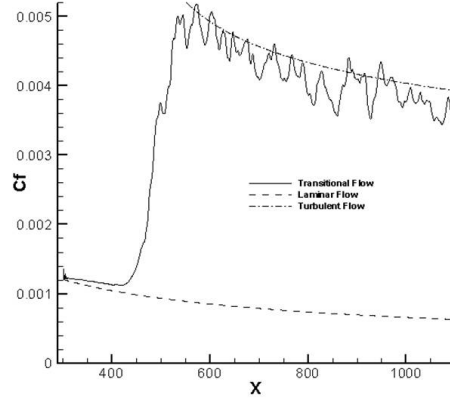
The skin friction coefficient calculated from the time-averaged and spanwise-averaged profile on a coarse and fine grid is displayed in Figure 5. The spatial evolution of skin friction coefficients of laminar flow is also plotted out for comparison. It is observed from these figures that the sharp growth of the skin-friction coefficient occurs after  $x \approx 450\delta_{in}$ , which is defined as the "onset point". The skin friction coefficient after transition is in good agreement with the flat-plate theory of turbulent boundary layer by Cousteix in 1989 (Ducros, [33]). Figures 5(a) and 5(b) also show that we get grid convergence in skin friction coefficients.

### 2.2.3 Comparison with Log Law

Time-averaged and spanwise-averaged streamwise velocity profiles for various streamwise locations in two different grid levels are shown in Figure 6. The inflow velocity profiles at  $x=300.79\delta_{in}$  is a typical laminar flow velocity profile. At  $x=632.33\delta_{in}$ , the mean velocity profile approaches a turbulent flow velocity profile (Log law). This comparison shows that the velocity profile from the DNS results is turbulent flow velocity profile and the grid convergence has been realized.

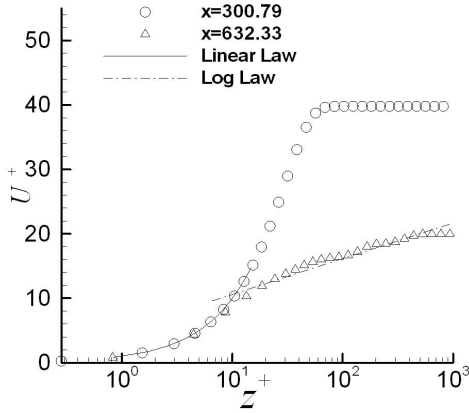


(a) Coarse Grids (960x64x121)

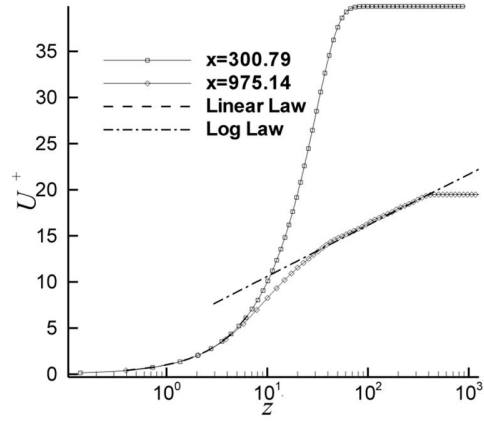


(b) Fine grid (1920x128x241)

Figure 5: Streamwise evolutions of the time-and spanwise-averaged skin-friction coefficient



(a) Coarse Grids (960x64x121)



(b) Fine grid (1920x128x241)

Figure 6: Log-linear plots of the time-and spanwise-averaged velocity profile in wall unit

## 2.2.4 Spectra and Reynolds stress (velocity) statistics

Figure 7 shows the spectra in  $x$ - and  $y$ - directions. The spectra are normalized by  $z$  at location of  $Re_x = 1.07 \times 10^6$  and  $Y^+ = 100.250$ . In general, the turbulent region is approximately defined by  $Y^+ > 100$  and  $y/\delta < 0.15$ . In our case, The location of  $y/\delta = 0.15$  for  $Re_x = 1.07 \times 10^6$  is corresponding to  $Y^+ \approx 350$ , so the points at  $Y^+ = 100$  and  $250$  should be in the turbulent region. A straight line with slope of  $-3/5$  is also shown for comparison. The spectra tend to tangent to the  $k^{-(\frac{5}{3})}$  law.

Figure 8 shows Reynolds shear stress profiles at various streamwise locations, normalized by square of wall shear velocity. There are 10 streamwise locations starting from leading edge to trailing edge are selected. As expected, close to the inlet at  $Re_x = 326.8 \times 10^3$  where the flow is laminar, the values of the Reynolds stress is much smaller than those in the turbulent region. The peak value increases with the increase of  $x$ . At around  $Re_x = 432.9 \times 10^3$ , a big jump is observed, which indicates the flow is in transition. After  $Re_x = 485.9 \times 10^3$ , the Reynolds stress profile becomes close to each other in the turbulent region. So for this case, we can consider that the flow transition starts after  $Re_x = 490 \times 10^3$ .

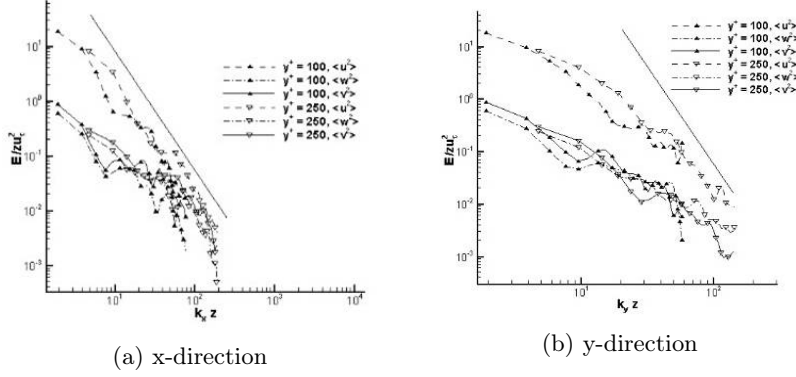


Figure 7: Spectra in x and y directions

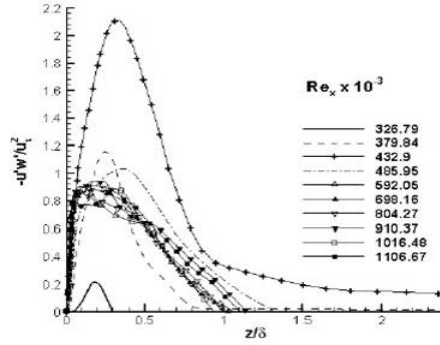


Figure 8: Reynolds stress

### 2.2.5 Comparison with Other DNS

Although we cannot compare our DNS results with those given by Borodulin et al (2002) quantitatively, we still can find that the shear layer structure are very similar in two DNS computations in Figure 9.

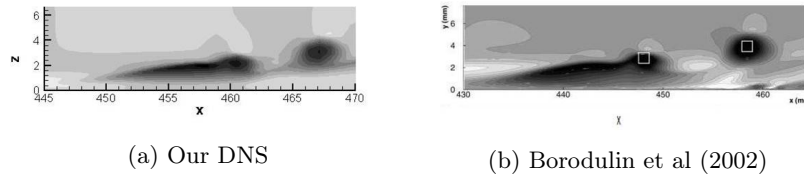


Figure 9: Qualitatively Comparison of contours of streamwise velocity disturbance  $u$  in the  $(x, z)$ -plane (Light shades of gray correspond to high values)

### 2.2.6 Comparison with Experiment

By this  $\lambda_2$ -eigenvalue visualization method, the vortex structures shaped by the nonlinear evolution of T-S waves in the transition process are shown in Figure 11. The evolution details are briefly studied in our previous paper (Chen et al [17]) and the formation of ring-like vortices chains is consistent with the experimental work (Lee C B and Li R Q, 2007, Figure 10) and previous numerical simulation by Rist and his co-authors (Bake et al 2002).

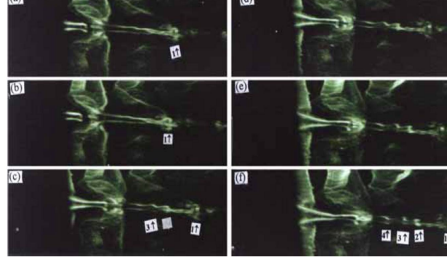


Figure 10: Evolution of the ring-like vortex chain by experiment (Lee et al, 2007)

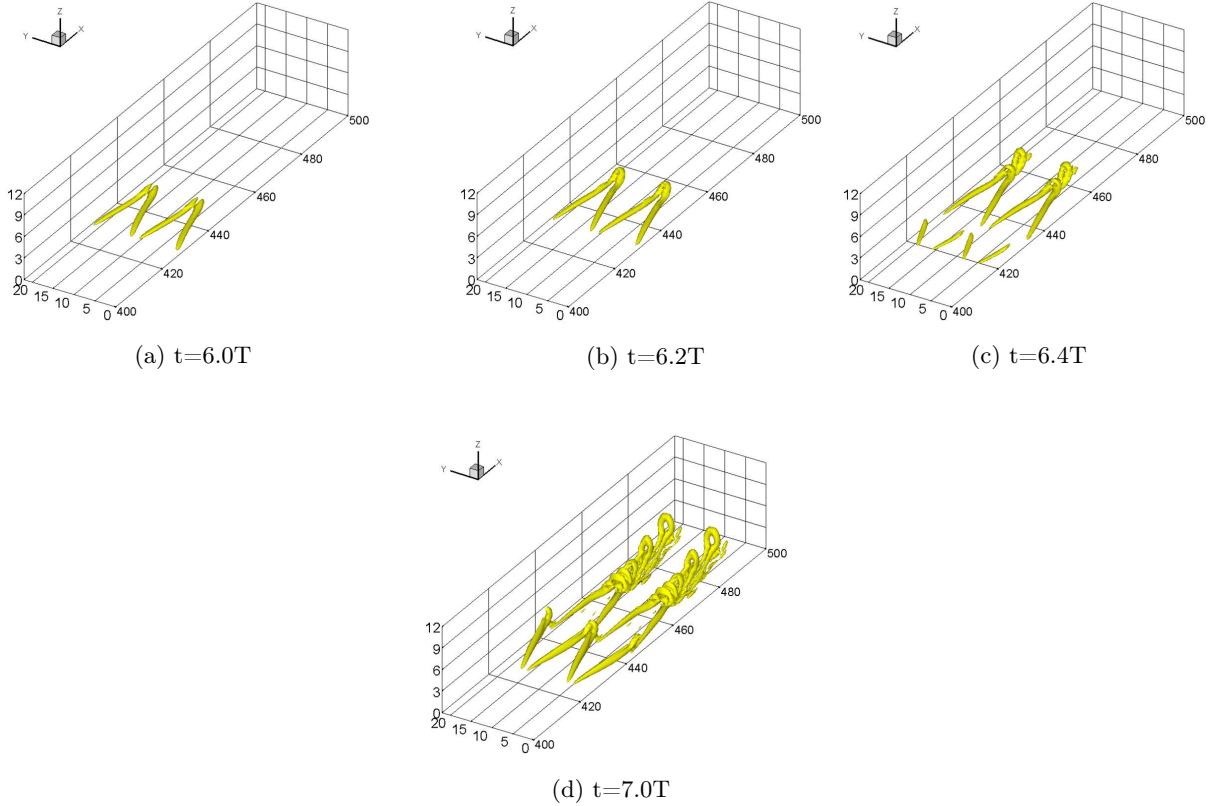


Figure 11: Evolution of vortex structure at the late-stage of transition(Where is the period of T-S wave)

### 2.2.7 U-shaped vortex in comparison with experimental results

Figure 12(a) (Guo et al, [3]) represents an experimental investigation of the vortex structure including ring-like vortex and barrel-shaped head (U-shaped vortex). The vortex structures of the nonlinear evolution of T-S waves in the transition process are given by DNS in Figure 12(b). By careful comparison between the experimental work and DNS, we note that the experiment and DNS agree with each other in a detailed flow structure comparison. **This cannot be obtained by accident, but provides the following clues:** 1) Both DNS and experiment are correct 2) Disregarding the differences in inflow boundary conditions (random noises VS enforced T-S waves) and spanwise boundary conditions (non-periodic VS periodic) between experiment and DNS, the vortex structures are same 3) No matter K-, H- or other types of transition, the final vortex structures are same 4) There is a universal structure for late boundary layer transition 5) turbulence has certain coherent structures (CS) for generation and sustenance.

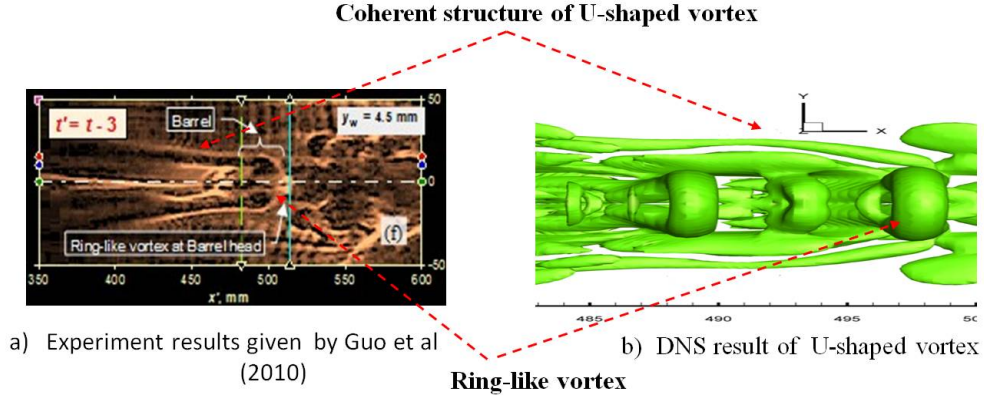


Figure 12: Qualitative vortex structure comparison with experiment

All these verifications and validations above show that our code is correct and our DNS results are reliable.

### 3 Observation and Analysis by Our DNS

Following observations have been made and reported by our previous publications [17, 18, 19, 20, 21, 22, 23, 24, 25, 26, 27, 28, 29, 30, 35, 36].

#### 3.1 Mechanism of large coherent vortex structure

Late boundary transition starts from the formation of the first vortex ring. Ring-like vortices play a vital role in the transition process of the boundary layer flow and must be studied carefully.

##### 3.1.1 Vortex rings in flow field (Chen et al [20])

According to Helmholtz vorticity conservation law, the vortex tube cannot have ends inside the flow field. The only form of vortex tube existing inside the flow field must be ring with or without legs on the boundaries (Figure 13)

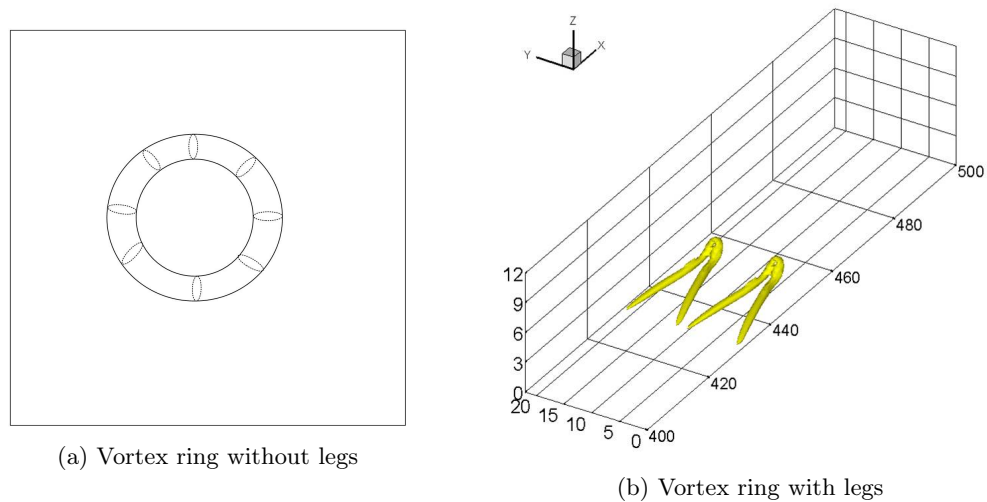


Figure 13: Vortex rings with or without legs

### 3.1.2 Mechanism of first ring-like vortex formation (Chen et al [19])

The ring shape of first ring-like vortex is caused by the interaction between the prime streamwise vortices and secondary streamwise vortices (Figure 14), which is quite different from one given by Moin et al (1986). The ring-like vortex is located at the edge of the boundary layer or in other words located in the inviscid zone ( $z = 3.56, U = 0.99U_e$ ). The vortex ring is perpendicularly standing and the shape of the ring is almost perfectly circular, which will generate the strongest downwash sweeps (Figures 14 and 15). More important, no vortex "pinch off" is observed.

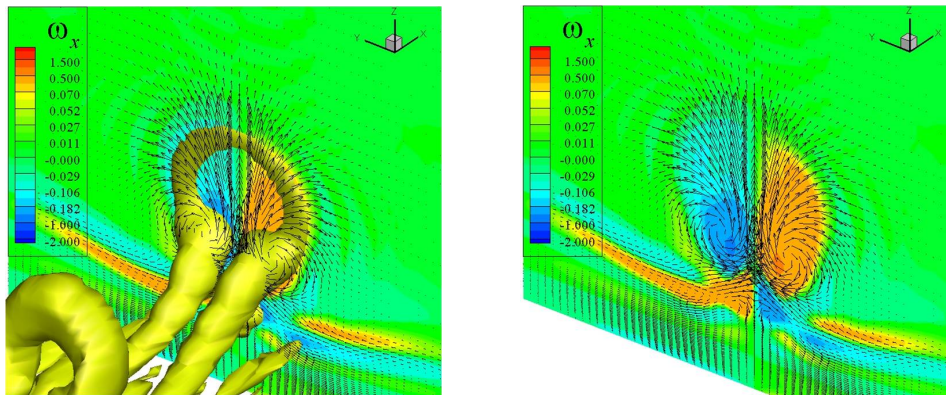


Figure 14: Formation processes of first ring-like vortex

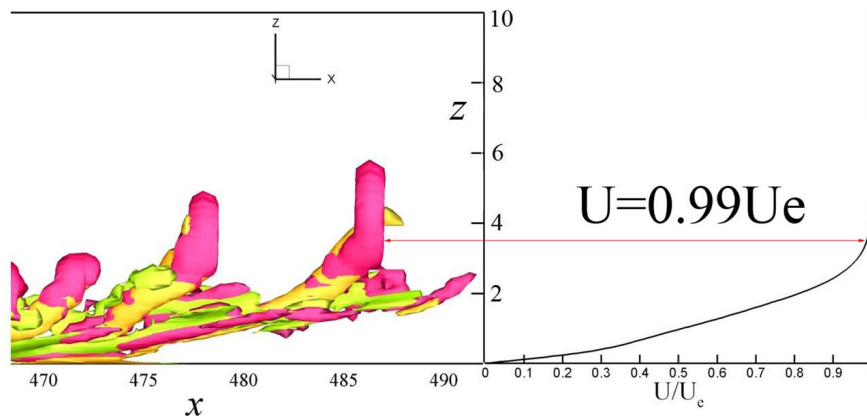


Figure 15: The shape and position of ring-like vortices in boundary layer ( $z = 3.56, U = 0.99U_e$ )

### 3.1.3 Mechanism of multiple ring formation

The ejection by rotation of the primary vortex legs brings low speed flow from lower boundary layer up and forms a cylinder-like momentum deficit zone in the middle of the two legs (green in Figure 16). The momentum deficit zone is also located above the legs and forms shear layers due to the stream-wise velocity difference between surrounding high speed flow and low speed flow in the deficit zone. These shear layers are not stable and multiple ring-like vortices (yellow in Figure 16) are generated by the shear layers one by one (Figure 17). This process must satisfy the Helmholtz vorticity conservation and the primary streamwise vorticity must be reduced when a new spanwise-oriented ring is formed (Figure 18). Different from Borodulin et al (2002), neither "vortex breakdown and reconnection" nor "Crow theory" is observed by our new DNS.

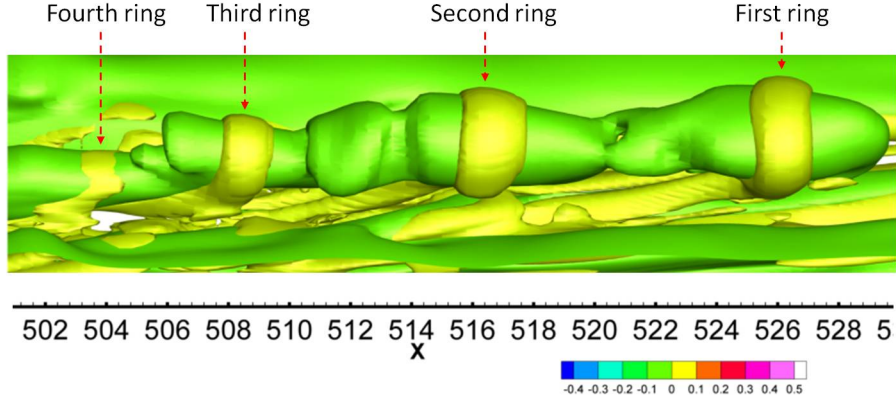


Figure 16: Three-dimensional momentum deficit and multiple ring-like vortex formation

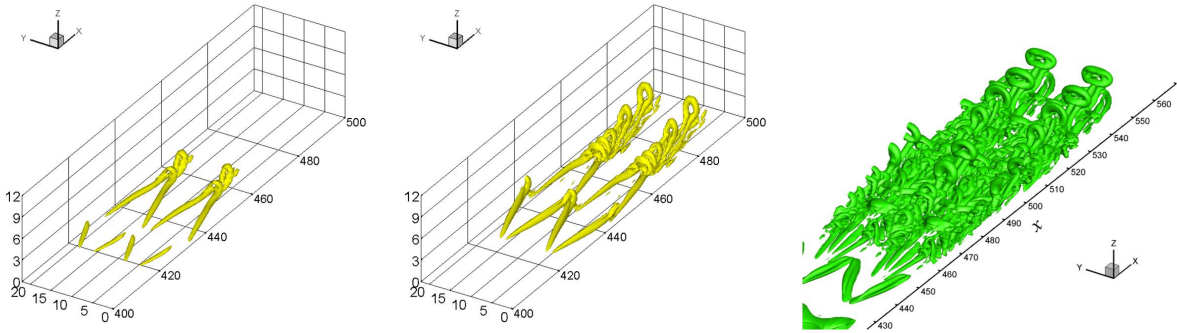


Figure 17: Multiple ring formation

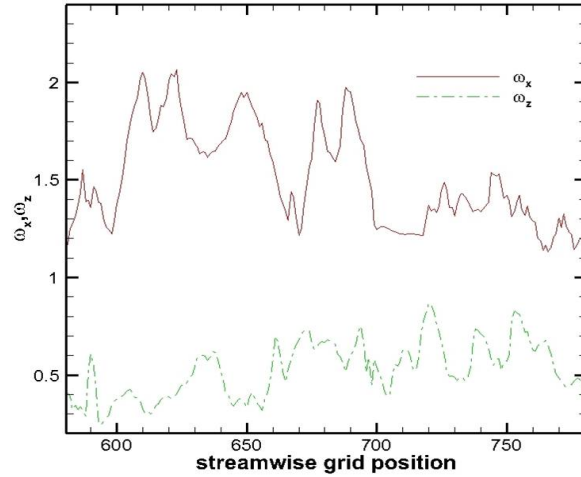


Figure 18: Maximum streamwise and spanwise vorticity along x-coordinate (Helmholtz vorticity conservation)

### 3.1.4 Primary, Secondary and U-shaped vortex (Lu et al, [28])

U-shaped vortex is part of large coherent vortex structure and is generated by secondary vortices which are induced by the primary vortex. Being different from Guo et al ([3]), the U-shaped vortex is not a wave

and is not induced by second sweeps and positive spikes. Actually, the U-shaped vortex is a tertiary (not secondary) vortex with same vorticity sign as the original ring legs (Figures 19 and 20). In addition, the U-shaped vortices serve as additional channels to supply vorticity to the multiple ring structure (Lu et al [29]).

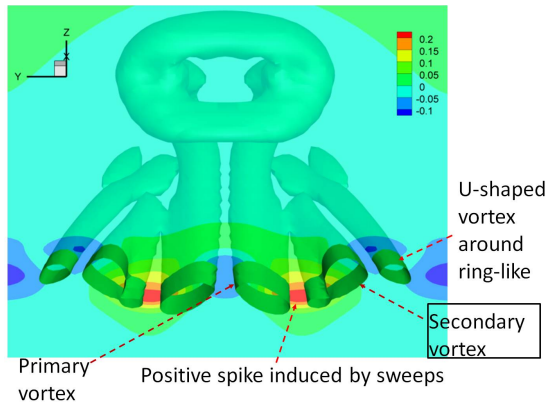


Figure 19: U-shaped vortex with streamwise velocity perturbation contour

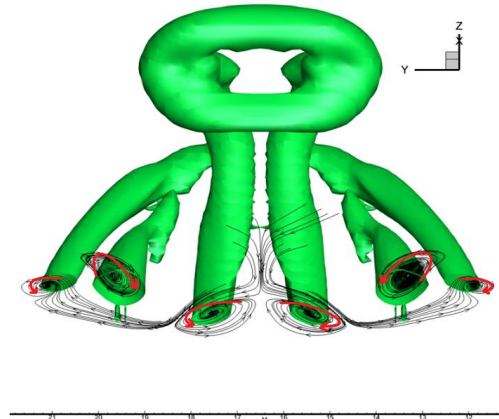


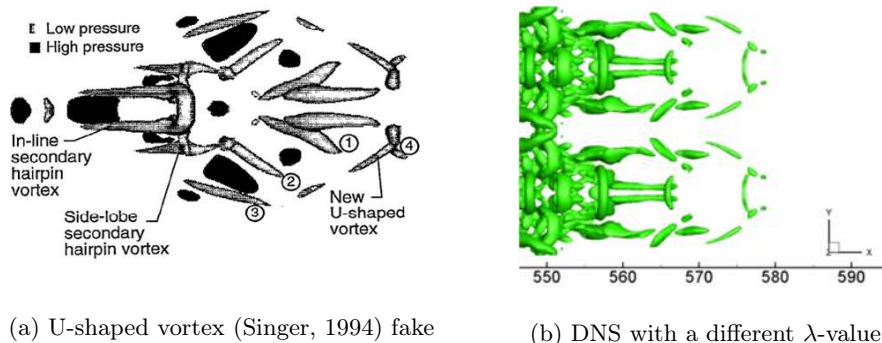
Figure 20: Isosurface of  $\lambda_2$  and streamtrace at  $x = 530.348\delta_{in}$

### 3.2 Mechanism of small length vortices generation

Turbulence has two features: 1) Small length vortices; 2) Non-symmetric structure (Randomization)

#### 3.2.1 Vortex breakdown to turbulence is challenged (Liu et al, [25, 26])

In the new DNS (Liu et al, [20, 21]), it has been observed that the multiple vortex structure is a quite stable structure and never breaks down. Previously reported "vortex breakdown" is either based on 2-D visualization or made by using low pressure center as the vortex center (Figure 21(a)). We can use a different  $\lambda_2$  value to get similar "vortex breakdown" (Figure 21(b)), which is faked. Here, we define vortex as a tube with a rotated core and iso-surfaces of constant vorticity flux. However, there is no evidence that the vortex breaks down. Let us look at the head of the so-called "turbulence spot" from different directions of view (Figures 22). Due to the increase of the ring (bridge) number and vorticity conservation, the leading rings will become weaker and weaker until they cannot be detected, but they never break down (see Figure 23).



(a) U-shaped vortex (Singer, 1994) fake

(b) DNS with a different  $\lambda$ -value

Figure 21: Formation processes of first ring-like vortex

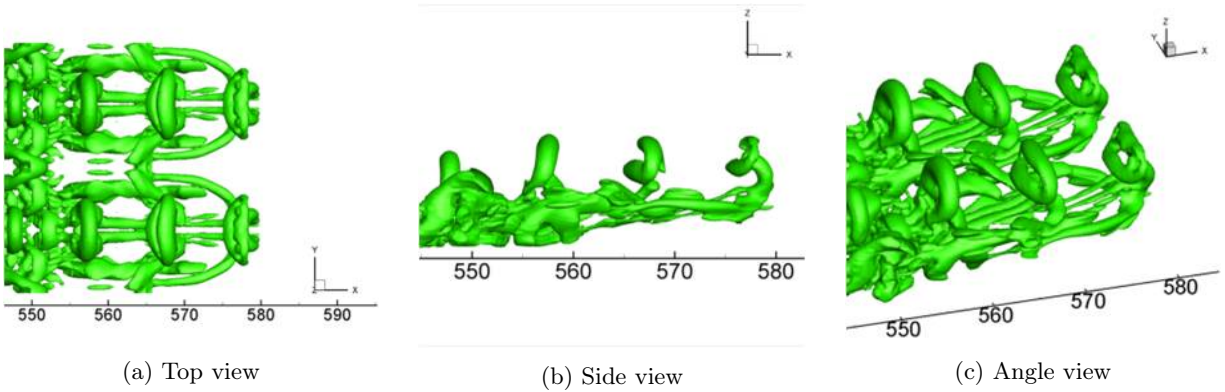


Figure 22: View of young turbulence spot head from different directions ( $t=8.8T$ )

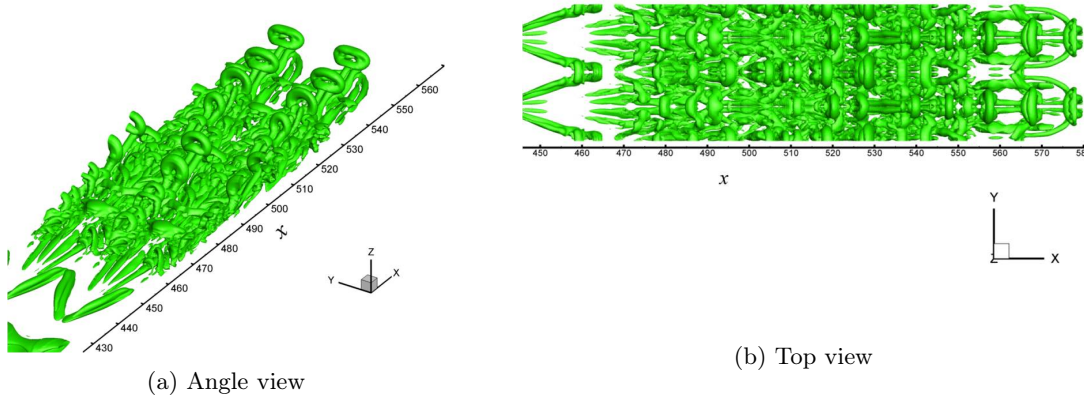


Figure 23: 3-D angle view and 2-D top view of the young turbulence spot ( $t=8.8T$ )

### 3.2.2 Mechanism of small length scale (turbulence) generation - by "shear layers" (Liu et al, [26]; Lu et al, [28])

The question will be raised that where the small length scales come from if the small vortices are not generated by "vortex breakdown"? Since we believe that the small vortices are generated by shear layers near the wall surface, we take snap shots in the direction of view from the bottom to top (Figure 24). The evidence provided by our new DNS confirms that the small length scale vortices are generated near the bottom of the boundary layer. Being different from classical theory which believes turbulence is generated by "vortex breakdown", our new DNS found that all small length scales (turbulence) are generated by high shear layers (HS) near the bottom of the boundary layers (near the laminar sub-layers). There is no exception. When we look at the later stage of flow transition at  $t=15T$ , we can see that all small length scales are located around the high-shear layers, especially at those near the wall surface (Figures 25-26).

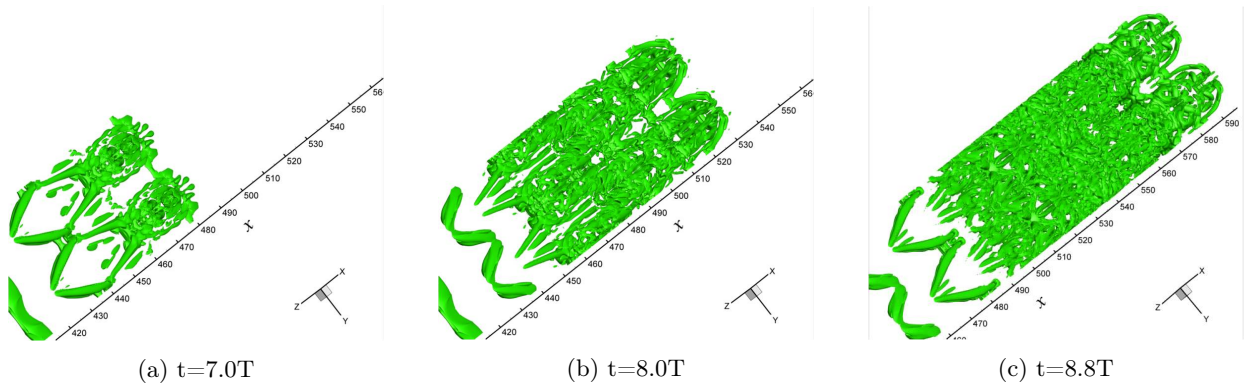


Figure 24: Small length scale vortex generation at different time steps (view up from bottom): small length scale vortices are generated by the solid wall near the ring necks from the beginning to the end

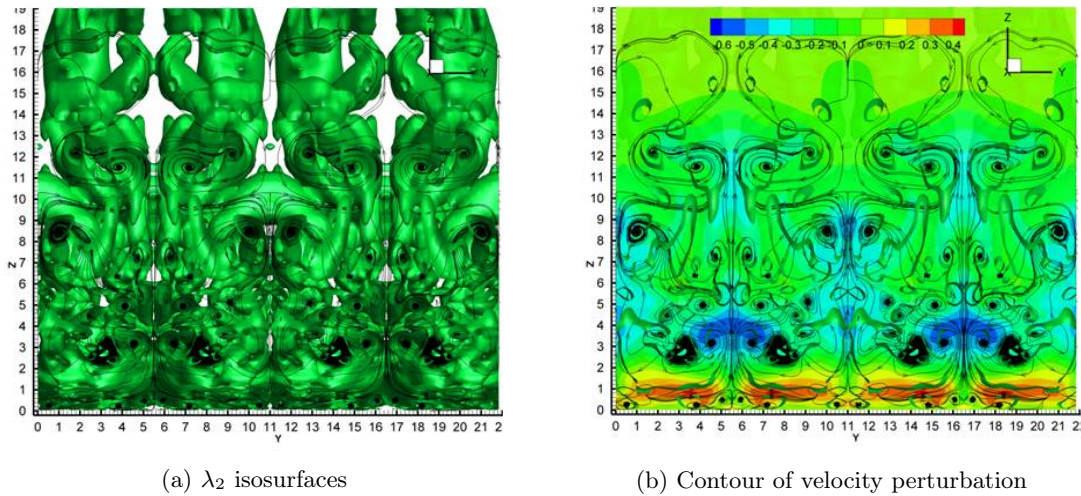


Figure 25: Visualization of isosurface  $\lambda_2$  and velocity perturbation at  $x=508.633$  for  $(Y, Z)$ -Plane  $t=15T$

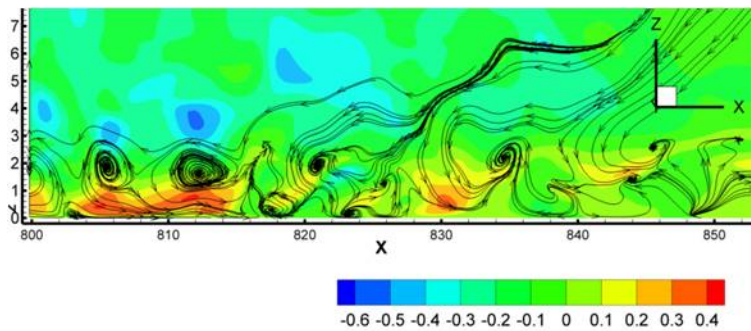


Figure 26: Visualization of isosurface  $\lambda_2$  and velocity perturbation at  $y=4$  for  $(X, Z)$ -Plane  $t=15T$

### 3.2.3 High shear layer formation by sweeps (Liu et al, [26])

Experiment and our numerical results have confirmed that there is a second sweep excited by every ring-like vortex (Figure 27). Combined with the first sweep generated by the original  $\lambda$  vortex legs, it forms strong positive spikes which generate strong high shears at the bottom of the boundary layer (red in Figure 28).

Figures 29 and 30 are contours of isosurface of  $\lambda_2$  and velocity perturbation at  $x=508.66$ . The second sweep movement induced by ring-like vortices working together with first sweep will lead to huge energy and momentum transformation from high energy inviscid zones to low energy zones near the bottom of the boundary layers and we can observe that **all small length scales are generated under the high speed region corresponding to high shear layers between the positive spike (momentum increment) and solid wall surface.**

### 3.2.4 Multiple level sweeps and multiple level negative and positive spikes (Lu et al, [28])

The positive spikes (momentum increment) could generate new ring-like vortices. The new ring-like vortices can further generate new sweeps and form new positive spikes (Figure 31) at the location which are very close to the bottom of the boundary layer (laminar sub-layer). The new positive spike could induce new smaller vortex rings by unstable shear layers. These multilevel sweeps and multilevel negative and positive spikes provide channels for energy transfer from the inviscid area (high energy area) down to the bottom (low energy area). **This is the mechanism why turbulence can be generated and sustained. This mechanism can be interpreted as a universal mechanism for both transitional and turbulent flow in a boundary layer.**

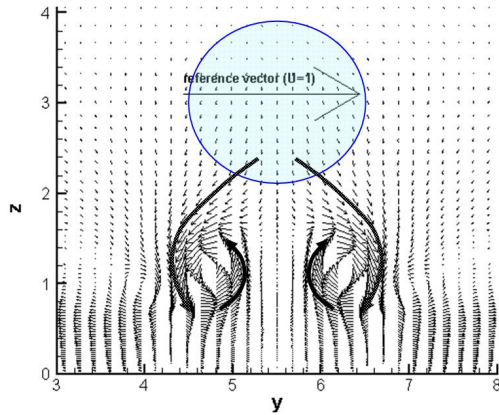


Figure 27: Velocity vector field

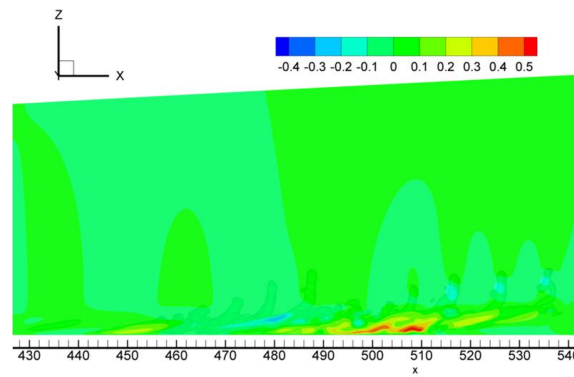


Figure 28: Vorticity distribution at  $x=508.633$

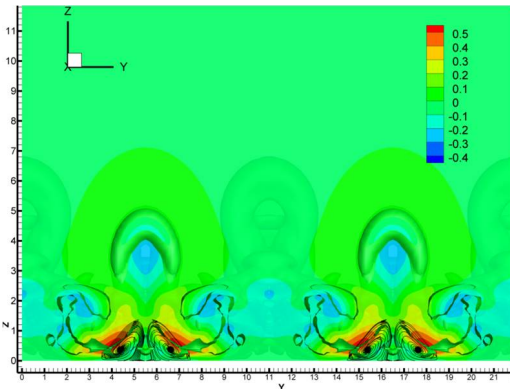


Figure 29: isosurface of  $\lambda_2$  and velocity at  $x=508.66$

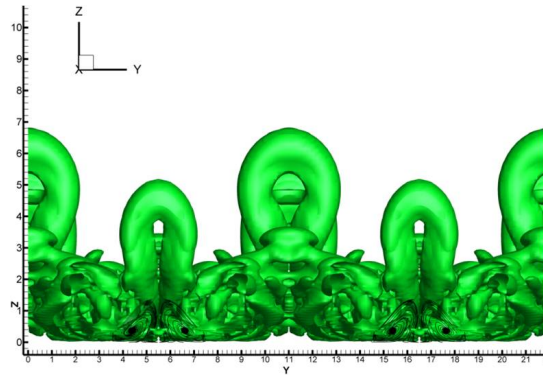


Figure 30: isosurface of  $\lambda_2$  and stream traces at  $x=508.66$

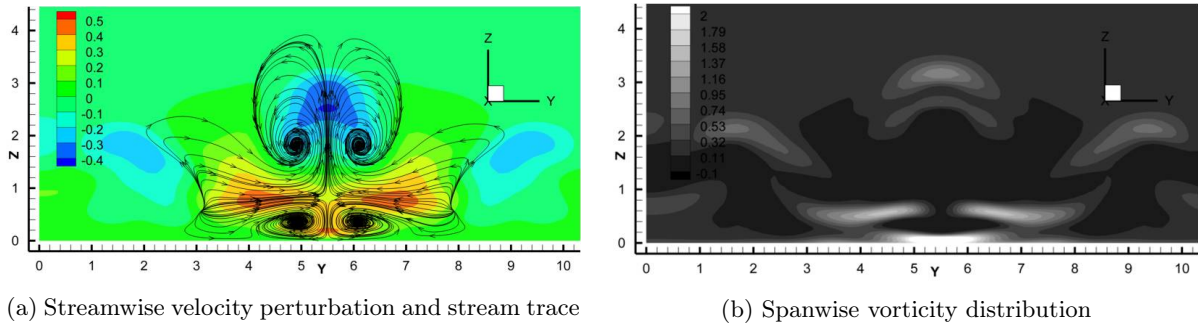


Figure 31: (a) Multilevel sweeps (b) multilevel positive spikes

### 3.2.5 Energy transfer paths and universal turbulence spot structure (Lu et al [28])

Figure 32 and 33 are sketches describing energy transfer and likely universal turbulence structure

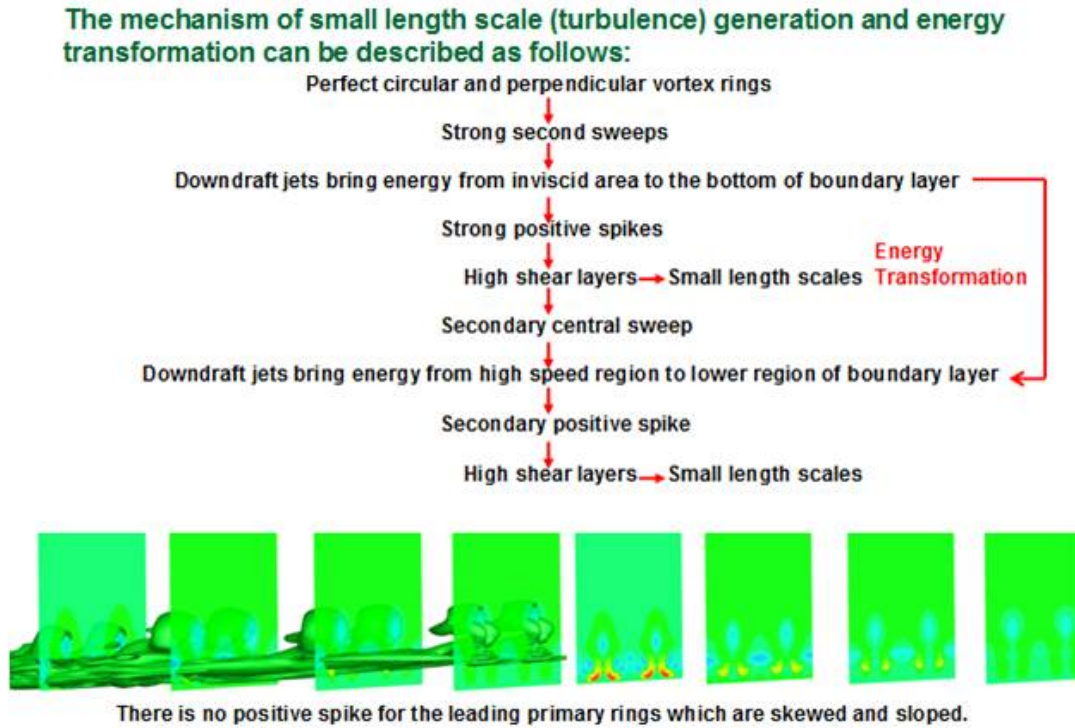


Figure 32: Energy transfer paths and universal structure for turbulence

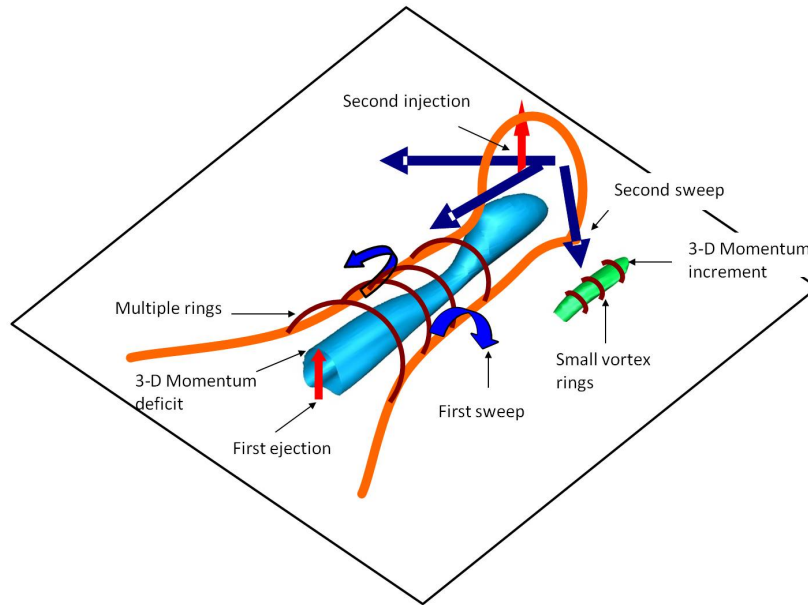


Figure 33: Sketch of mechanism of multiple rings formation and small vortices formation

### 3.2.6 Surface friction

Figure 34 is a time and spanwise averaged surface friction coefficient (CF). From the figure, it is clearly seen that there is a jump starting at  $x=430$  which indicates an onset of flow transition and reach a maximum value at  $x=508.663$ . It is conventionally believed that the CF is large in the turbulent area and small in the laminar area due to the strong mixing in turbulent flow. That is the reason why most turbulence models are formulated based on change of turbulent viscosity. However, from Figure 34, it is easy to find that the CF reaches maximum in a laminar area and is not directly related to mixing. Further analysis found the viscosity is not changed for incompressible flow, but the shear layer is changed sharply when the first and second sweeps caused positive spikes (momentum increment), HS layers and consequent small vortices generations. The velocity gradients suddenly jump to a very large level in the laminar sub-layer and then the CF becomes very large. Therefore, the CF jump is not caused by mixing or viscosity coefficients increase, but is, pretty much, caused by velocity gradient jump due to small vortices formation.

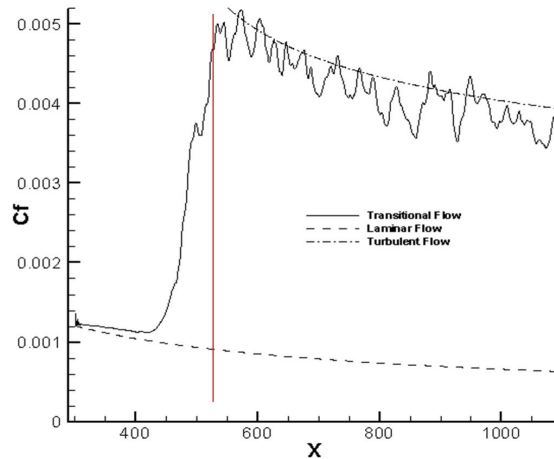


Figure 34: Maximum CF at  $x=508.633$  (Laminar)

### 3.3 Loss of symmetry (Randomization)

The existing theory (Meyer et al, [34]) believes that the flow randomization in DNS is caused by the background noises and removal of periodic boundary conditions. They believe that randomization starts from loss of symmetry, which is caused by background noise. According to that theory, the ring tip is affected first, which rapidly influences the small length scale structure. This will lead to loss of symmetry and randomization for the whole flow field quickly.

However, what we observed in our new DNS is that the loss of symmetry starts from middle level rings (Figure 35) while the top and bottom rings are still symmetric (Figure 36). The non-symmetric structure of middle level rings will influence the small length scale at the bottom quickly. The change of symmetry in the bottom of the boundary layer is quickly spread to up level through ejections. This will lead to randomization of the whole flow field. Therefore, the internal instability of multiple level ring overlapping structure, especially the middle ring cycles, is a critical reason for flow randomization, but mainly not the background noise. In addition, the loss of symmetry starts in the middle of the streamwise direction, not the inflow and not the outflow (Figure 37a). As mentioned, we did not change the periodic boundary conditions and the solution is still periodic in the spanwise direction (period= $2\pi$ ). In addition, we did not add any additional background noise or inflow perturbation. However, we found that the flow lost symmetry first and then was randomized step by step (see Figure 38-41). The flow was first periodic (period= $\pi$ ) and symmetric in the spanwise direction, but then lost symmetry in some areas, and finally everywhere. It was periodic with a period of  $\pi$ , same as the inflow, but changed with a period of  $2\pi$ . The flow is still periodic because we enforced the periodic boundary condition in the spanwise direction with a period of  $2\pi$ . This means the flow does not only have  $\sum_{k=0}^n a_k \cos(2ky)$  but also have  $\sum_{k=0}^n a_k \sin(2ky)$  which is newly generated. Meanwhile, flow lost periodicity with period= $\pi$ , but has to be periodic with period= $2\pi$  (Figure 40 and 41), which we enforced. Since the DNS study is focused on the mechanism of randomization and the DNS computation only allows use two periods in the spanwise direction, we consider that the flow is randomized when the symmetry is lost and period is changed from  $\pi$  to  $2\pi$  (Figure 38 and 39):

$$f(y) = \sum_{k=0}^n a_k \cos(2ky) + \sum_{k=0}^{n-1} a_k \sin(2ky) + \sum_{k=0}^{n-1} a_k \cos(2ky + y) + \sum_{k=0}^{n-1} a_k \sin(2ky + y)$$

In real flow, there is no such a restriction of periodic boundary condition in the spanwise direction.

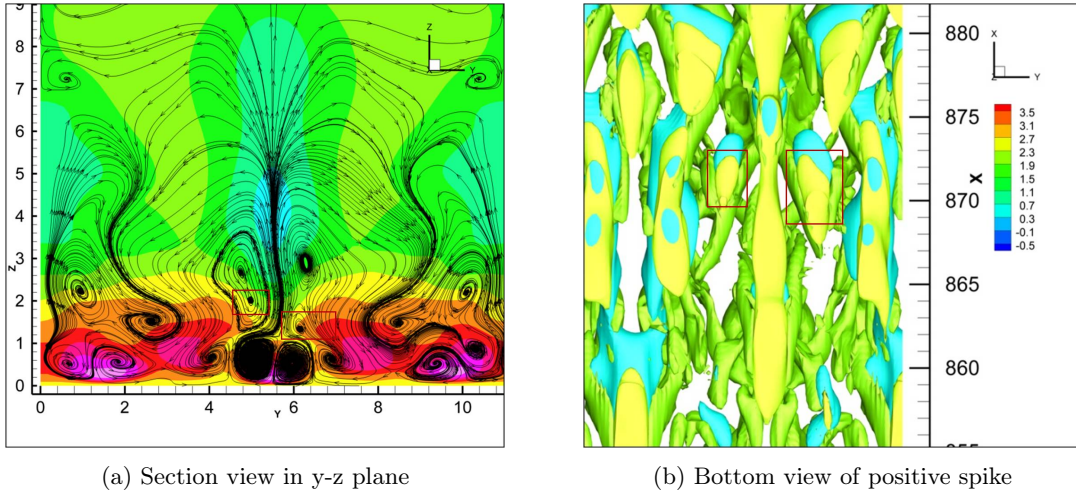


Figure 35: The flow lost symmetry in second level rings and bottom structure at  $t=15.0T$

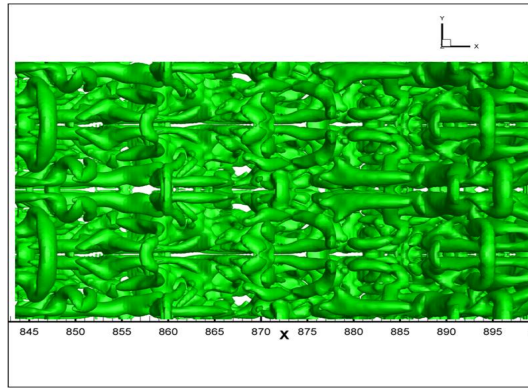
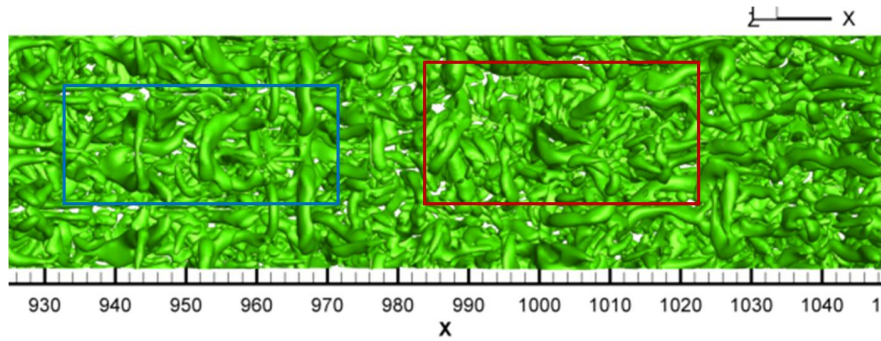
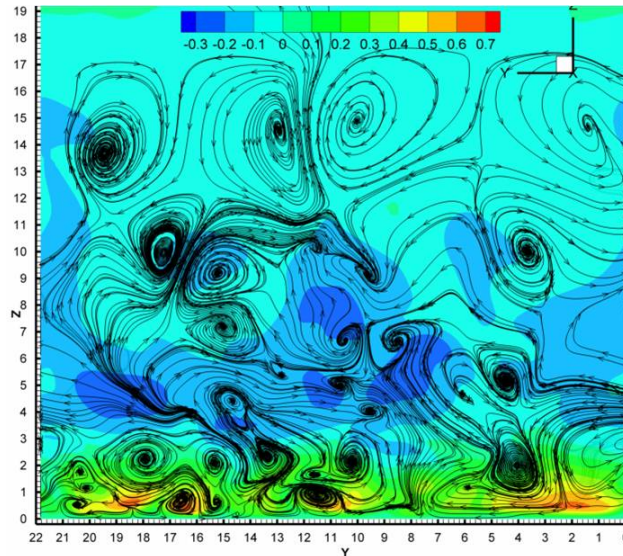


Figure 36: The top ring structure is still symmetric at  $t=15.0T$



(a) Top ring structure lost symmetry (blue area is symmetric but red area is not)



(b) Symmetry loss in the whole section of y-z plane

Figure 37: The whole flow field lost symmetry at  $t=21.25T$

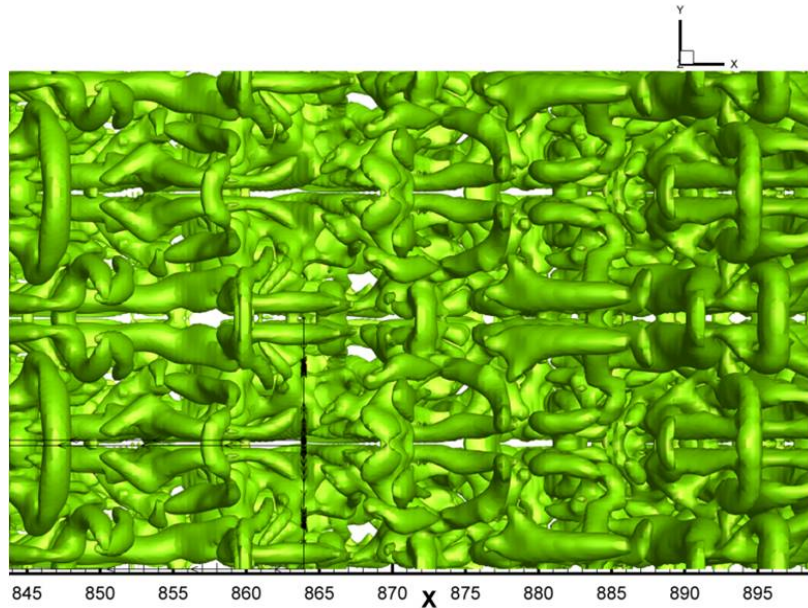


Figure 38: Whole domain is symmetric and periodic  $\times \cos(2y)$  (the period  $=\pi$ ; spanwise domain is  $-\pi < y < \pi$ )

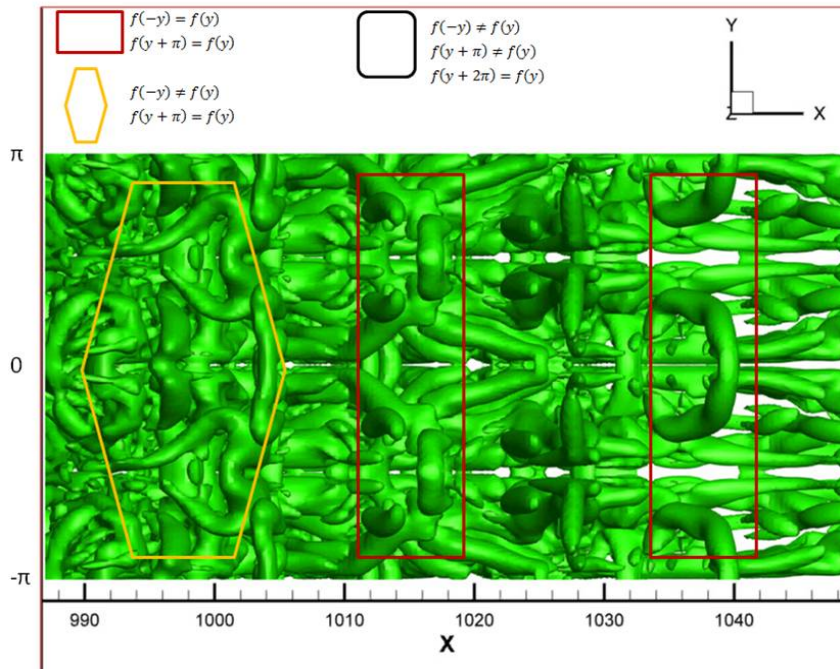


Figure 39: Symmetric and asymmetric - red rectangular: periodic and symmetric at  $y = -\pi/2, 0, \pi/2$ , i.e.  $f(-\pi/2) = f(-\pi/2 + y)$ ,  $f(-y) = f(y)$ ,  $f(\pi/2 - y) = f(\pi/2 + y)$ ; yellow diamond: periodic,  $f(y + \pi) = f(y)$ , period  $=\pi$ ; but asymmetric  $f(-y) \neq f(y)$ ; the spanwise domain is  $-\pi < y < \pi$

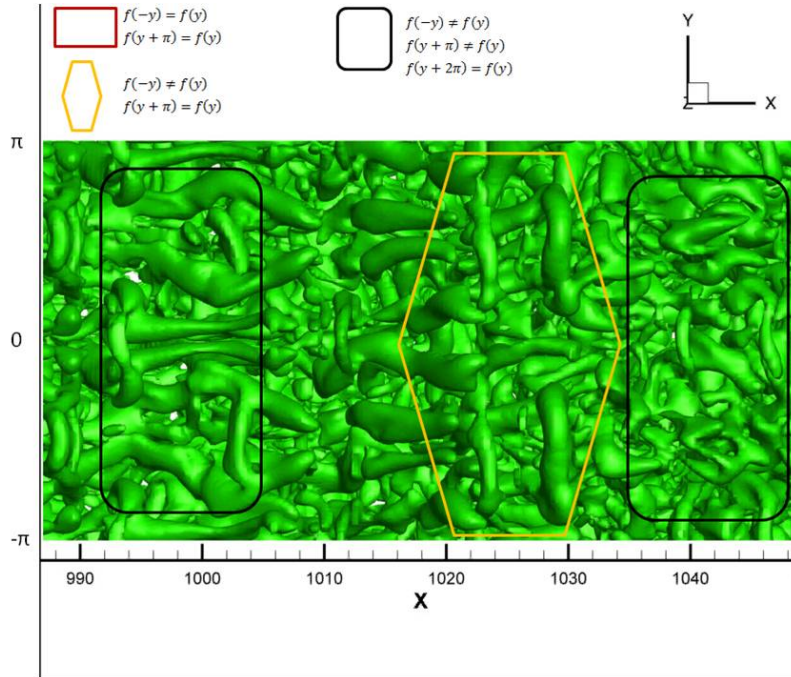


Figure 40: Periodic but asymmetric - yellow diamond: periodic, period= $\pi$ ; black box: periodic but period= $2\pi$ ; the spanwise domain is  $-\pi < y < \pi$

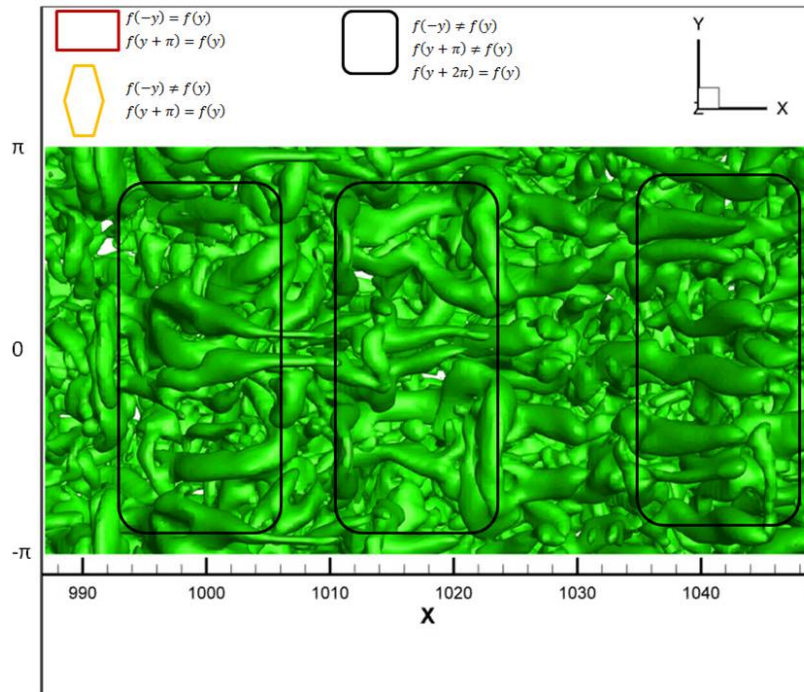


Figure 41: Periodic but asymmetric -black boxes: periodic but asymmetric (period= $2\pi$ ); the spanwise domain is  $-\pi < y < \pi$

## 4 Summary of Our DNS Findings

Since turbulence generation and sustenance are one of the top secret in nature, this research will bring significant impact on fundamental fluid mechanics as the classical theory and dominant concepts on late flow transition and turbulence structure are challenged. Table 2 gives a comparison of classical theory and currently dominant conclusions with the observation by our DNS:

Table 2: comparison of classical theory and our DNS

Topic	Classical or Existing Theory	Observation of Our DNS
Turbulence generation	By "Vortex Breakdown"	Not by "Vortex Breakdown" but by shear layer instability
First ring generation	Self-induced, deformed, inclined and pinched-off	By counter-rotated vortices interaction, circular, perpendicular, no pinch-off
Multiple ring structure	"Crow theory" or breakdown and then re-connected	No breakdown, not "Crow theory" but momentum deficit caused by ejection, vorticity conservation
Multiple level high shears	No report	By multiple level sweeps and ejections
Energy transfer channel	Energy transfers from larger vortices to smaller one through "vortex breakdown" without dissipation until viscosity	From inviscid flow down to bottom
turbulence sustenance		by multilevel sweeps
U-shaped vortex	Head wave, secondary vortex, by second sweep, newly formed, breakdown	Not head wave, tertiary vortex, by secondary vortex, existing from beginning, never breakdown
Randomization	Background noise, starting from the top ring and then going down to the bottom	Internal property, starting from second level rings in the middle, affects bottom and then up to affect top rings.
Coefficients of friction	Turbulent flow has large friction due to strong boundary layer mixing	Depending only on velocity profile changes in laminar sub-layer, no matter turbulent or laminar
Richardson eddy cascade	Classical theory	Not observed
Vortex breakdown	Classical theory	Not observed
Kolmogorov scale	Classical theory	Smallest length scale should be determined by minimum shear layer instability

## Acknowledgments

This work was supported by AFOSR grant FA9550-08-1-0201 supervised by Dr. John Schmisser and the Department of Mathematics at University of Texas at Arlington. The authors are grateful to Texas Advanced Computing Center (TACC) for providing computation hours. This work is accomplished by using Code DNSUTA which was released by Dr. Chaoqun Liu at University of Texas at Arlington in 2009.

## References

- [1] R. J. Adrian. *Hairpin vortex organization in wall turbulence*. Physics of Fluids, 2007.
- [2] X. Wu and P. Moin. *Direct numerical simulation of turbulence in a nominally zero-pressure gradient flat-plate boundary layer*. JFM, 630:5-41, 2009.
- [3] H. Guo and V.I. Borodulin and Y.S. Kachanov and C. Pan and J.J. Wang and S.F. Wang. *Nature of sweep and ejection events in transitional and turbulent boundary layers*. J. of Turbulence, 2010.
- [4] T. Mullin. *Turbulent times for fluids*. New Scientist, 1989.

- [5] P. A. Davidson, *Turbulence: An Introduction for Scientists and Engineers*, Oxford University Press, 2004.
- [6] Kolmogorov and N. Andrey. *The local structure of turbulence in incompressible viscous fluid for very large Reynolds numbers*. Proceedings of the Royal Society of London, Series A: Mathematical and Physical Sciences, 434:9-13, 1991.
- [7] U. Frisch. *Turbulence: The Legacy of A. N. Kolmogorov*, Cambridge University Press, 1995.
- [8] T. Herbert. *Secondary Instability of Boundary Layer*. Annu. Rev.Fluid Mech., 20:487-526, 1988.
- [9] Y. S. Kachnaov. *Physical Mechanisms of Laminar-Boundary-Layer Transition*. Annu. Rev.Fluid Mech., 26:411-482, 1994.
- [10] L. Kleiser and T. A. Zang. *Numerical simulation of transition in wall-bounded shear flows*. Annu.Rev.Fluid Mech, 23:495-537, 1991.
- [11] D. Sandham and L. Kleiser. *The late stages of transition in channel flow*. J. Fluid Mech., 245:319-348, 1992.
- [12] U. Rist and Y.S. Kachanov. Numerical and experimental investigation of the K-regime of boundary-layer transition. *Laminar-Turbulent Transition* (Berlin: Springer), 1995.
- [13] V. I. Boroduhn and V.R. Gaponenko and Y. S. Kachanov. *Late-stage transition boundary-Layer structure: direct numerical simulation and experiment*. Theoret.Comput.Fluid Dynamics, 15:317-337, 2002.
- [14] S. Bake and D. Meyer and U. Rist. *Turbulence mechanism in Klebanoff transition: a quantitative comparison of experiment and direct numerical simulation*. J.Fluid Mech, 459:217-243, 2002.
- [15] Y.S. Kachanov. *On a universal mechanism of turbulence production in wall shear flows*. 86:1-12, 2003.
- [16] M. Piller and E. Stalio. *Compact finite volume schemes on boundary-fitted grids*. Journal of Computational physics, 227:4726-4762, 2008.
- [17] L. Chen and X. Liu and M. Oliveira and D. Tang and C. Liu. *Vortical Structure, Sweep and Ejection Events in Transitional Boundary Layer*. Science China, Series G, Physics, Mechanics,Astronomy, 39(10):1520-1526, 2009.
- [18] L. Chen and X. Liu and M. Oliveira and C. Liu. *DNS for ring-like vortices formation and roles in positive spikes formation*. AIAA Paper 2010-1471, 2010.
- [19] L. Chen and D. Tang and P. Lu and C. Liu. *Evolution of the vortex structures and turbulent spots at the late-stage of transitional boundary layers*. Science China, Physics, Mechanics and Astronomy, 53(1):1-14, 2010.
- [20] L. Chen and C. Liu. *Numerical Study on Mechanisms of Second Sweep and Positive Spikes in Transitional Flow on a Flat Plate*. Journal of Computers and Fluids, 40:28-41, 2011.
- [21] L. Chen and X. Liu and D. Tang and C. Liu. *volution of the vortex structures and turbulent spots at the late-stage of transitional boundary layers*. Science of China, Physics, Mechanics & Astronomy, 54(5):986-990, 2011.
- [22] C. Liu and L. Chen. *Study of mechanism of ring-like vortex formation in late flow transition*. AIAA Paper 2010-1456, 2010.
- [23] X. Liu and L. Chen and M. Oliveira and D. Tang and C. Liu. *DNS for late stage structure of flow transition on a flat-plate boundary layer*. AIAA Paper 2010-1470, 2010.
- [24] X. Liu and Z. Chen and C. Liu. *Late-Stage Vortical Structures and Eddy Motions in Transitional Boundary Layer Status*. Chinese Physics Letters, 27(2), 2010.
- [25] C. Liu and L. Chen and P. Lu. *New Findings by High Order DNS for Late Flow Transition in a Boundary Layer*. J. of Modeling and Simulation in Engineering, open access journal and copy right is kept by authors, 2011.
- [26] C. Liu and L. Chen. *Parallel DNS for vortex structure of late stages of flow transition*. J. of Computers and Fluids, 45:129-137, 2011.
- [27] C. Liu. *Numerical and Theoretical Study on "Vortex Breakdown"*. International Journal of Computer Mathematics, Website [<http://www.tandfonline.com/doi/abs/10.1080/00207160.2011.617438>], 2010.
- [28] C. Liu and L. Chen and P. Lu and X. Liu. *Study on Multiple Ring-Like Vortex Formation and Small Vortex Generation in Late Flow Transition on a Flat Plate*. Theoretical and Numerical Fluid Dynamics, Website [<http://www.springerlink.com/content/e4w2q465840nt478/>], 2010.
- [29] P. Lu and C. Liu. *Numerical Study of Mechanism of U-Shaped Vortex Formation*. AIAA Paper 2011-0286, 2011.
- [30] P. Lu and C. Liu. *DNS Study on Mechanism of Small Length Scale Generation in Late Boundary Layer*

- Transition*. AIAA Paper 2011-0287, 2011.
- [31] J. Jeong and F. Hussain. *On the identification of a vortex*. J. Fluid Mech, 285:69-94, 1995.
  - [32] L. Jiang and C. L. Chang and M. Choudhari and C. Liu. *Cross-Validation of DNS and PSE Results for Instability-Wave Propagation*. AIAA Paper 2003-3555, 2003.
  - [33] F. Duros and P. Comte and M. Lesieur. *Large-eddy simulation of transition to turbulence in a boundary layer developing spatially over a flat plate*. J.Fluid Mech, 326:1-36, 1996.
  - [34] D.G.W. MEYER and U. RIST and M.J. KLOKER. *Investigation of the flow randomization process in a transitional boundary layer*. High Performance Computing in Science and Engineering, 3:239-253, 2003.
  - [35] P. Lu and M. Thampa and C. Liu. *Numerical Study on Randomization in Late Boundary Layer Transition*. AIAA paper, 2012.
  - [36] J. Cai and L. Jiang and C. Liu. *Large Eddy Simulation of Wing Tip Vortex in the Near Field*. International Journal of CFD, 22(5):289-330, 2008.